

Spin transport in organics and organic spin devices

Z.G. Yu, M.A. Berding and S. Krishnamurthy

Abstract: The authors present a theory to describe spin transport across a polymer sandwiched between magnetic contacts and propose organic spin devices based on this theory. It is found that even a weak magnetic field can significantly modify spin transport in polymers through spin precession. This sensitivity can be exploited to design ultrasensitive magnetometers and low-power magnetic-field-effect transistors. It is shown that, at room temperature, the organic magnetometers are capable of detecting sub-nanotesla magnetic fields, and the I–V characteristics of the magnetic-field-effect transistors can be strongly modified by magnetic fields of a few gauss with response times of a few nanoseconds.

1 Introduction

In spin-based electronics (spintronics), information is carried by the electron spin. Semiconductor spintronic devices have attracted considerable attention (see [1] and references therein), since the discovery of long spin lifetimes in semiconductor structures [2]. Compared with inorganic materials, organics have much longer spin lifetimes because of the vanishing spin-orbit couplings, suggesting that organic materials have significant potential for novel spintronic devices. Recently, strong magnetoresistances and large spin injection have been observed in $\text{La}_{0.7}\text{Sr}_{0.3}\text{MnO}_3$ (LSMO)/sexithienyl (T_6)/LSMO and LSMO/8-hydroxyquinolate aluminum (Alq_3)/Co structures even at room temperature [3, 4]. T_6 and Alq_3 are two widely used materials in organic electronics. Theoretical studies of spin-dependent transport in magnet/organic material/magnet structures have just begun, and a consistent understanding is still lacking. A systematic theoretical study of spin injection, spin manipulation and spin detection in organic structures is required to understand the experiments and to design new organic spintronic devices.

Organic electronic devices, including light-emitting diodes and field-effect transistors, have been the subjects of intense research in the last decade because they have processing and performance advantages for low-cost and/or large-area applications (see, for example, [5]). On the other hand, the low carrier mobility (10^{-8} – $10\text{ cm}^2/\text{Vs}$) in organics limits their application for high-speed devices such as computer processors. The arena of organic electronic devices is in the applications that exploit unique properties in organics, such as large-area processing, mechanical flexibility, tunable light emission, chemical sensing interactions, and biocompatibility.

Similarly, organic spintronic devices have some unique applications that are inaccessible to inorganic spintronic devices. In this paper, we will show that both the low carrier mobility and the long spin lifetime in organics can be

exploited to achieve room-temperature ultrasensitive magnetic sensors and low-power magnetic-field-effect transistors (MFETs). These devices use dense films of conjugated polymers or organic molecules and are distinct from molecular electronic devices, where carriers traverse individual molecules coherently [6]. There is a huge demand on low-magnetic-field ($<10^{-6}$ gauss) sensors for medical applications and military surveillance as well as on earth-field (10^{-6} – 1 G) sensors for navigation and geology [7]. Many of these applications currently rely on superconducting quantum interference devices (SQUIDs) that require cooling at cryogenic temperatures. We will show that the proposed organic magnetic sensors are capable of detecting a magnetic field as weak as 10^{-9} G at room temperature. This extraordinary sensitivity, together with other favourable attributes of organic devices, including light weight, flexibility, low cost and biocompatibility, suggests that the organic spintronic devices will play an important role in magnetic sensing and in detection of biological targets in the near future.

2 Spin transport in organics

Despite recent important progress in experimentally demonstrating strong magnetoresistance and large spin injection in organic structures, a comprehensive understanding of these experiments is still unavailable. The major problem is that a consistent description of spin transport for organic structures is yet to be established. Existing theories for magnetic tunnelling junctions or for metallic layered structures are frequently applied to organic structures. These theories are either invalid or inadequate for spin transport in organics. A complete and appropriate description of spin transport in organics should include the following factors: (i) spin transport across organic structures is diffusive rather than due to tunnelling; (ii) electric fields in organic structures are very strong because organics are typically undoped or lightly doped; and (iii) noncollinear structures should be consistently incorporated [3].

We consider spin transport in a magnet/organic/magnet structure. In such a structure, the magnet work functions and their relative position with respect to the electron- and hole-polaron levels in the polymer determine which type of carrier (electron or hole) is dominantly responsible for

© IEE, 2005

IEE Proceedings online no. 20050043

doi:10.1049/ip-cds:20050043

Paper first received 23rd February and in revised form 18th March 2005

The authors are with SRI International, Menlo Park, California 94025, USA

E-mail: zhi-gang.yu@sri.com

transport [5]. In this paper, we focus on a single-carrier device in which the carriers are holes (electron devices can be analysed similarly), which is appropriate for LSMO/T₆/LSMO and LSMO/Alq₃/Co structures.

When a voltage is applied to a magnet/polymer/magnet structure, a spin-polarised current is injected into the polymer from the magnets, giving rise to spin accumulation in the polymer. To consider spin precession and non-collinear configurations, where spin accumulation can be along any direction, we use a 2×2 density matrix in spin space to describe the carrier distribution, $\hat{\rho}^P = \rho_0^P \hat{\mathbf{1}} + \hat{\boldsymbol{\sigma}} \cdot \boldsymbol{\rho}^P$. Here $\rho_0^P \hat{\mathbf{1}}$ is the equilibrium carrier distribution of the nonmagnetic polymer, and $\hat{\boldsymbol{\sigma}} = (\hat{\sigma}_x, \hat{\sigma}_y, \hat{\sigma}_z)$ are Pauli matrices.

The spin-polarised current in the polymer consists of two contributions, drift and diffusion,

$$\hat{\mathbf{j}}^P = \hat{\rho}^P e v \mathbf{E} - e D \nabla \hat{\rho}^P \quad (1)$$

where v is the carrier mobility and D the diffusion constant in the polymer. The drift-diffusion-type model has been widely used to model (spin-independent) charge transport in organic electronic devices and has proven to be reliable and accurate [5]. Here, we neglect the possible magnetic-field effect on the orbital motion (Hall effect), which is reasonable in polymers with low carrier mobilities. In a nondegenerate system, v and D are connected via Einstein's relation $v/eD = 1/k_B T$. The continuity equation for each component of the density matrix in the presence of a magnetic field \mathbf{B} reads as

$$\frac{\partial \hat{\rho}^P}{\partial t} = \frac{\hat{\rho}^P - \hat{\rho}_0^P \hat{\mathbf{1}}}{\tau_S} - \frac{1}{e} \nabla \cdot \hat{\mathbf{j}}^P + \frac{i}{\hbar} \left[\hat{\rho}^P, -\frac{g \mu_B}{2} (\hat{\boldsymbol{\sigma}} \cdot \mathbf{B}) \right] \quad (2)$$

where τ_S is the spin relaxation time, g the gyromagnetic factor of the material and μ_B the Bohr magneton. To emphasise the spin-dependent part in carrier transport, as a simplification, we assume that the charge distribution inside the polymer is homogeneous, and $\nabla \rho_0^P = 0$, $\nabla \cdot \mathbf{E} = 0$, although a more accurate description requires self-consistently solving Poisson's equation together with transport equations [5]. This assumption can be justified when the length scale associated with charge inhomogeneity, the Debye length, is much shorter than the spin-diffusion length, as in the structures in [3]. In steady state we obtain

$$\nabla^2 \boldsymbol{\rho}^P - \frac{e \mathbf{E}}{k_B T} \cdot \nabla \boldsymbol{\rho}^P - \frac{\rho^P}{L^2} - \mathbf{b} \times \boldsymbol{\rho}^P = 0 \quad (3)$$

where $\mathbf{b} \equiv g \mu_B \mathbf{B} / \hbar D$ and $L = \sqrt{D \tau_S}$. This equation provides a consistent description of spin drift and spin precession in polymers. A similar equation for semiconductors was derived recently from the Boltzmann equation [8]. The spin precession effect, controlled by the ratio \mathbf{b}/D , is particularly important in polymers because of their small diffusion constants (low mobilities). In the absence of spin drift, by scaling all lengths in terms of L , we see that D does not explicitly influence spin transport. However, the spin drift term in (3) introduces another length scale $k_B T / |eE|$, which makes D directly affect the spin transport behaviour.

For systems homogeneous in the lateral direction all quantities depend on only one co-ordinate (x). We obtain the general solution to (3) in such a system

for a magnetic field along $\mathbf{B} = B (\sin \theta \cos \phi, \sin \theta \sin \phi, \cos \theta)$:

$$\begin{aligned} \boldsymbol{\rho}^P(x) = & C_1 v_0 e^{\lambda_1 x} + C_2 v_0 e^{\lambda_2 x} \\ & + C_3 (v_1 e^{\lambda_3 x} \cos \lambda_4 x - v_2 e^{\lambda_3 x} \sin \lambda_4 x) \\ & + C_4 (v_1 e^{\lambda_3 x} \sin \lambda_4 x + v_2 e^{\lambda_3 x} \cos \lambda_4 x) \\ & + C_5 (v_1 e^{\lambda_5 x} \cos \lambda_4 x + v_2 e^{\lambda_5 x} \sin \lambda_4 x) \\ & + C_6 (v_1 e^{\lambda_5 x} \sin \lambda_4 x - v_2 e^{\lambda_5 x} \cos \lambda_4 x), \\ v_0 = & (\sin \theta \cos \phi, \sin \theta \sin \phi, \cos \theta), \\ v_1 = & (\cos \theta \cos \phi, \cos \theta \sin \phi, -\sin \theta), \\ v_2 = & (\sin \phi, -\cos \phi, 0), \\ \lambda_{1,2} = & eE / 2k_B T \pm \gamma, \\ \lambda_{3,5} = & eE / 2k_B T \pm \sqrt{\gamma^2 + \sqrt{\gamma^4 + |b|^2} / \sqrt{2}}, \\ \lambda_4 = & \sqrt{-\gamma^2 + \sqrt{\gamma^4 + |b|^2} / \sqrt{2}} \end{aligned}$$

where $\gamma^2 = (eE / 2k_B T)^2 + 1/L^2$. If the magnetic-field-induced spin precession is absent, the general solution becomes $\boldsymbol{\rho}^P(x) = \mathbf{A}_1 e^{x/L_u} + \mathbf{A}_2 e^{-x/L_d}$. Here, \mathbf{A}_1 and \mathbf{A}_2 are two constant vectors, and L_u and L_d are the upstream and downstream spin diffusion lengths [9–11]:

$$L_{u,d} = (\pm |eE| / 2k_B T + \gamma)^{-1} \quad (4)$$

The spin transport distance (L_d) is greatly enhanced by the electric field (current).

The density matrix $\hat{\rho}^P$ is related to the electrochemical potential $\hat{\mu}^P$ in the polymer. For nondegenerate systems with carriers following the Boltzmann distribution, we find $\hat{\mu}^P = \mu_0^P \hat{\mathbf{1}} + \hat{\boldsymbol{\sigma}} \cdot \boldsymbol{\mu}^P$ with

$$\boldsymbol{\mu}^P = \frac{k_B T}{e} \frac{\boldsymbol{\rho}^P}{2|\boldsymbol{\rho}^P|} \left[\ln \left(1 + \frac{|\boldsymbol{\rho}^P|}{\rho_0^P} \right) - \ln \left(1 - \frac{|\boldsymbol{\rho}^P|}{\rho_0^P} \right) \right] \quad (5)$$

where μ_0^P is determined by $d\mu_0^P/dx = -J/\sigma_p = -E$, with σ_p the conductivity of the polymer and $J = \text{Tr} \hat{\mathbf{j}}^P$ the total current. Thus $\mu_0^P(x) = -Ex + C_0$, where C_0 is a constant.

The two magnets in a magnet/polymer/magnet are described in [12, 13]. These magnets can be regarded as magnetic reservoirs in local equilibrium at chemical potentials $\mu_{\mathcal{L},\mathcal{R}}^M$, which is diagonal in spin space $\hat{\mu}_{\mathcal{L},\mathcal{R}}^M = \mu_{\mathcal{L},\mathcal{R}}^M \hat{\mathbf{1}}$. Here $\mathcal{L}(\mathcal{R})$ denotes the left (right) magnet. The direction of the magnetisation in each magnet is described by the unit vector $\mathbf{m}_{\mathcal{L},\mathcal{R}}$. The current from the left contact to the polymer is [12, 13]

$$\begin{aligned} \hat{\mathbf{j}}^C(0) = & G^\uparrow \hat{u}_{\mathcal{L}}^\uparrow [\hat{\mu}_{\mathcal{L}}^M - \hat{\mu}^P(0)] \hat{u}_{\mathcal{L}}^\uparrow + G^\downarrow \hat{u}_{\mathcal{L}}^\downarrow [\hat{\mu}_{\mathcal{L}}^M - \hat{\mu}^P(0)] \hat{u}_{\mathcal{L}}^\downarrow \\ & - G^{\uparrow\downarrow} \hat{u}_{\mathcal{L}}^\uparrow \hat{\mu}^P(0) \hat{u}_{\mathcal{L}}^\downarrow - G^{\downarrow\uparrow} \hat{u}_{\mathcal{L}}^\downarrow \hat{\mu}^P(0) \hat{u}_{\mathcal{L}}^\uparrow \end{aligned} \quad (6)$$

The current from the right contact to the polymer $\hat{\mathbf{j}}^C(d)$ can be written similarly. Here, we assume that carriers in the polymer are in quasi-equilibrium, which can be characterised by a spin-dependent electrochemical potential in the spin space $\hat{\mu}^P$. We emphasise that the polymer is nondegenerate and the relation between $\hat{\rho}$ and $\hat{\mu}$ in (5) is very different from that described in references [8, 9] for metals. Operators $\hat{u}_{\mathcal{L}}^{\uparrow(1)} = \frac{1}{2} [1 + (-)\hat{\boldsymbol{\sigma}} \cdot \mathbf{m}_{\mathcal{L}}]$ and $\hat{u}_{\mathcal{R}}^{\uparrow(1)} = \frac{1}{2} [1 + (-)\hat{\boldsymbol{\sigma}} \cdot \mathbf{m}_{\mathcal{R}}]$ project spins on the magnetisation directions of the magnets. These equations can be regarded as a generalised Ohm's law in the spin space. G^\uparrow (G^\downarrow) is the electron conductance in the magnet with spin parallel (antiparallel) to the magnetisation direction. $G^{\uparrow\downarrow} = \text{Re} G^{\uparrow\downarrow} + i \text{Im} G^{\uparrow\downarrow}$ is the mixing conductance, which

measures the transport capability of spins oriented perpendicular to the magnetisation direction. In the diffusive regime G^\uparrow and G^\downarrow can be calculated through $\sigma_c^{\uparrow(\downarrow)}/L_c$, where L_c is the length of the contact and $\sigma_c^{\uparrow(\downarrow)}$ is the up-spin (down-spin) conductivity of the contact. It is required that $\text{Re}G^{\uparrow\downarrow} \geq (G^\uparrow + G^\downarrow)/2$ [11].

The requirement that the currents be continuous provides the following boundary conditions: (i) $\hat{j}^C(0) = \hat{j}^P(0)$ and (ii) $-\hat{j}^C(d) = \hat{j}^P(d)$. These two 2×2 matrix equations completely determine the eight unknowns $-C_i (i=0, 1, \dots, 6)$ and $\mu_L^M - \mu_R^M$ (voltage drop), for a given current J . Having solved these equations, we can calculate the total resistance of the structure $R = (\mu_L^M - \mu_R^M)/J$. All numerical calculations presented here are for room temperature. We adopt in our calculations the parameters appropriate for the LSMO/T₆/LSMO structures, which have been obtained by fitting theoretical results to the experimental measurements [14, 15]. $L = 50$ nm, $\sigma_p = 10^{-6} (\Omega \text{cm})^{-1}$, $G^\uparrow = 10^5 \Omega \text{cm}^2$, $G^\downarrow = 10^{-2} \Omega \text{cm}^2$ and $G^{\uparrow\downarrow} = 0.7 \times 10^5 \Omega \text{cm}^2$.

First, we examine spin transport in the absence of spin precession. In Fig. 1, we depict the device resistance R as a function of relative angle Θ between the contact magnetisations ($\cos \Theta = \mathbf{m}_L \cdot \mathbf{m}_R$) at different electric fields (currents). The device size, $d = 200$ nm, is much larger than the spin diffusion length L . When the electric field is weak, the injected carriers from the left LSMO contact become unpolarised when they reach the right contact because $L_d \simeq L = 50$ nm $\ll d$, and therefore the resistance does not depend on magnetisation directions of the right LSMO contact. With increase of the electric field, we see that the total resistance becomes sensitive to the magnetisation directions of the LSMO contacts, which is due to the field-enhanced spin transport distance in the polymer (L_d), as shown in the inset of Fig. 1, which enables carriers to retain their spin polarisation when they reach the right LSMO contact.

Next we investigate the impact of spin precession on spin transport in magnet/polymer/magnet structures. We consider structures with $\mathbf{m}_{L,R}$ in the y - z plane, and spin precession is created by a transverse magnetic field along the x -direction. It is expected from (3) that even a weak magnetic field can strongly influence spin transport because

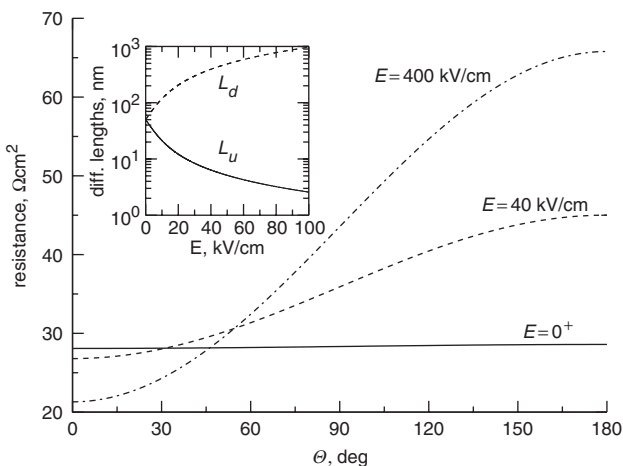


Fig. 1 Total resistance as function of angle between magnetisations of two LSMO contacts for device of $d = 200$ nm under different currents with fixed $G^{\uparrow\downarrow} = 70000 (\Omega \text{cm}^2)^{-1}$

Solid, dashed and dot-dashed lines correspond to $E = 0^+$, 40 and 400 kV/cm, respectively. The inset illustrates upstream (solid line) and downstream (dashed line) diffusion lengths as a function of electric field

of the low mobility in the polymer. Figure 2a delineates the device resistance as a function of transverse magnetic field, for a device of $d = 10$ nm ($L \gg d$) under a vanishing current ($E = 0^+$). We see that the resistance decreases with the applied magnetic field and that the change is particularly strong for an antiparallel configuration. In the absence of spin precession, the device resistance is large because either spin species must be the minority spin in one of the contacts for the antiparallel configuration. With a transverse magnetic field, the spin orientation of carriers will vary over the distance through spin precession, providing a channel connecting the majority spins in the two LSMO contacts, thereby reducing the resistance. Another effect of spin precession at weak electric fields (diffusive regime) is the reduction of spin accumulation at the interfaces, which occurs because carriers diffuse along random trajectories, and different trajectories lead to different precession angles. This effect is suppressed at high electric fields (drift regime).

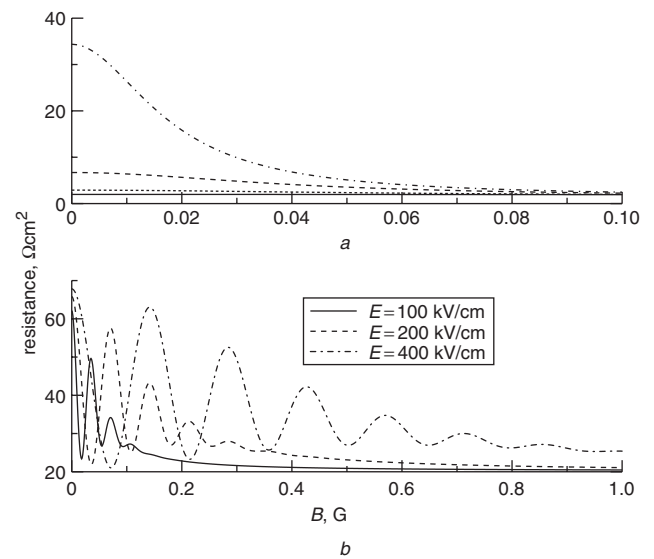


Fig. 2 Total resistance as function of transverse magnetic field
a Device of $d = 10$ nm with different Θ under $E = 0^+$. Solid, dotted, dashed and dot-dashed lines correspond to $\Theta = 0^\circ, 90^\circ, 135^\circ$, and 180° , respectively

b Device of $d = 200$ nm with $\Theta = 180^\circ$ under different electric fields. Solid, dashed and dot-dashed lines correspond to $E = 100, 200$, and 400 kV/cm, respectively. The mobility is $\nu = 10^{-5} \text{cm}^2/\text{Vs}$

Figure 2b shows the resistance of an antiparallel configuration with $d = 200$ nm as a function of transverse magnetic field at high electric fields. Under these electric fields, the spin transport distance is greatly enhanced by drift, $L_d \gg d$. This explains the strong magnetoresistance, even for $L \ll d$. We see that the device resistance displays a damped oscillating behaviour as the transverse magnetic field increases, and that the oscillating period is proportional to the strength of the electric field. We can understand the oscillation by noticing that spin drift due to electric field leads to a finite transit time, $\tau_D = d/\nu E$. The time scale of spin precession τ_P is determined by the Lamor frequency ω_L ($\tau_P \equiv 2\pi/\omega_L = 2\pi\hbar/g\mu_B B$). Thus the peaks of resistance occur when $\tau_D = n\tau_P (n = 1, 2, \dots)$, i.e. $B = n2\pi\hbar\nu E/g\mu_B d$ [16]. The damping is due to the reduction of spin accumulation at the interfaces because of spin precession. This oscillating resistance does not exist in a metallic system,

where spin drift is negligible ($\tau_D \rightarrow \infty$) (see Fig. 2a). We emphasise that the resistance is extremely sensitive to the transverse magnetic field and the spin transport behaviour can be modified in different ways by controlling the interplay between spin precession and spin drift.

3 Organic spin devices

The carrier mobility in organics is intrinsically low, which is often considered to be a burden that limits the speed of organic-based electronic devices. Organic spintronic devices will be competitive and useful only when they do not require high carrier mobility. In this Section, we show that *both* low mobilities and long spin lifetimes in organics can be exploited to make organic MFETs and ultrasensitive magnetometers.

Our design is based on the theory of spin transport in organic structures discussed in Section 2. According to this theory, spin-dependent transport in organics can be strongly modified by magnetic-field-induced spin precession. Spin precession is very sensitive to the magnetic field in the polymer, because the precession is controlled by the ratio B/D . Furthermore, extremely long spin relaxation times in polymers allow spin-polarised carriers to have ample time to precess without losing their spin coherence when they traverse the polymer. Another crucial ingredient in the device is that the half-metallic magnets, such as LSMO [17, 18], are used as contacts on which organics can be easily deposited, to ensure efficient spin injection into the polymer. Although spin precession has been exploited either electrically or optically in metals [19–21] and in semiconductors [16, 22, 23], the proposed organic devices are novel because the functions of these devices rely on unique material properties in organics.

The device structure is illustrated in Fig. 3. It consists of an organic film on top of an insulator contacted by two LSMO electrodes. A metal strip beneath the insulator may be needed if an electrically controlled magnetic field is desired for an MFET. The basic device operation can be described as follows. Consider a device structure with the magnetisations of two LSMO contacts being antiparallel. In the absence of a transverse magnetic field, the device resistance is large because either spin species (up or down) must be the minority spin in one of the contacts and neither up-spin nor down-spin carriers can traverse the device easily. When a transverse magnetic field is applied, the spin orientation of carriers will vary over the distance in the polymer (spin precession), which provides a channel connecting the majority spins in the two LSMO contacts, and the resistance is therefore reduced. The electric field also

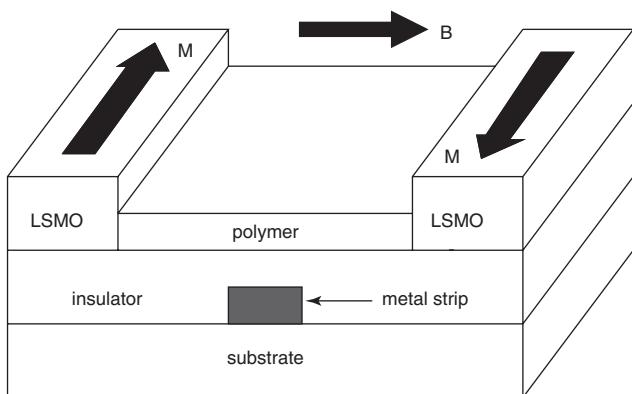


Fig. 3 Schematic device structure of organic MFET and magnetometer

strongly affects spin transport in the devices: (1) it considerably increases spin diffusion length through spin drift, and (2) it determines the transit time of injected carriers in the device and modifies the resistance through the ratio of the transit time and the spin precession time (determined by the magnetic field). The feasibility of fabricating these spin devices has been established by the recent experiments described in [3, 4]. In the proposed devices the magnetoresistance is achieved, not by changing the contact magnetisations, but by applying a transverse magnetic field (perpendicular to the contact magnetisations) to induce spin precession.

In Fig. 4 we plot the voltage drop V over a $d=200$ nm structure with antiparallely aligned LSMO contacts and its differential response, dV/dB , as a function of the transverse magnetic field with a constant current density, $J=0.4$ A/cm². The mobility is set to be 10^{-5} cm²/Vs. We see that, as the magnetic field increases, the voltage across the device displays a damped oscillating behaviour. The electric field in the device is $E=J/\sigma_p=4 \times 10^5$ V/cm. Under this electric field, the spin transport distance (downstream spin diffusion length) at room temperature is $L_d \approx 4000$ nm, which is longer than the device width. The oscillation in the magnetoresistance is attributed to the periodic spin precession angle within the carrier transit time, as discussed earlier. The damping is due to the reduction of spin accumulation at the interfaces because of spin precession [14, 15]. The differential response dV/dB measures the sensitivity of this device. We see that for some magnetic fields, dV/dB can be as high as 500 V/G. This remarkable value indicates that a magnetic field change as small as $\Delta B=10^{-9}$ G (0.1 pT) will give rise to a readily measurable voltage change of $0.5 \mu\text{V}$. Even at low magnetic fields around 10^{-5} G (1 nT), as shown in the inset of the Fig. 4, $dV/dB \approx 1$ V/G, corresponding to $\Delta B=0.05$ nT for a voltage change of $0.5 \mu\text{V}$. Thus, this organic structure is an ultrasensitive magnetometer that can detect both small magnetic fields and small magnetic-field differences at sub-nT levels. It is interesting to note that the sensitivity $dV/dB=500$ V/G at the bias of 10 V corresponds to $d(\Delta R/R)/dB=5000\%/G$, which is significantly greater than the values ($\leq 20\%/G$) in recently proposed magnetic sensors for detection of pT and fT magnetic fields [24–26], suggesting that the organic magnetometer, combined with clever circuitry design, is capable of detecting a even weaker magnetic field.

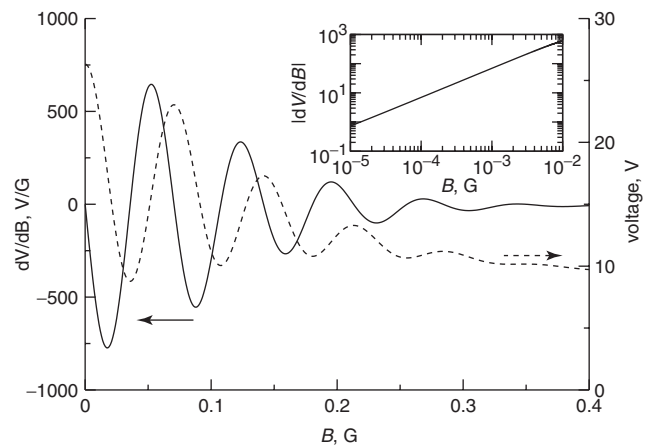


Fig. 4 Voltage (dashed line) and its differential response (solid line) as function of transverse magnetic field with constant current density $J=0.4$ A/cm² for antiparallel structure. The inset plots the differential response for small magnetic fields in logarithmic scale

In practice, the separation between the contacts, d , is not uniform throughout the device because of unavoidable contact roughness. However, as the ultrasensitive magnetometer is designed to detect extremely weak magnetic fields, i.e. within the first oscillating period (<0.05 G in Fig. 4), where the sensitivity dV/dB depends on the magnetic field almost linearly, the sensitivity will not be significantly compromised as long as the variation of d is relatively small.

The strong magnetic-field dependence of transport in these organic structures suggests that they can be used for low-power MFETs, where the I–V characteristics are modified by a magnetic field. As an efficient transistor requires a short response time, which is characterised by the transit time τ_R , we use a very high mobility for organics, $\nu = 1 \text{ cm}^2/\text{Vs}$ (as in pentacene), to describe MFETs. For such a high mobility, we estimate the spin diffusion length to be $L = 5000 \text{ nm}$ (assume that the spin lifetime has a value of 10^{-6} to 10^{-5} s and does not depend on the mobility) and the conductivity to be $\sigma_p = 10^{-2} (\Omega \text{ cm})^{-1}$. In Fig. 5 we plot transistor current-voltage curves of an antiparallel structure exposed to different transverse magnetic fields using these parameters. We see the modification of the I–V characteristics by different magnetic fields. These magnetic fields (≤ 10 G) are much weaker than the coercive field of the LSMO contacts (hundreds of G) and will not affect their magnetisations. Such transverse magnetic fields can also be created by supplying a current through the metal strip beneath the organic film, as shown in Fig. 3. The required current I can be estimated through $B = \mu_0 I / 2\pi r$, where r is the distance between the polymer and the metal strip and μ_0 the permeability. For $r = 10 \text{ nm}$, a current of $5 \mu\text{A}$ is needed to produce a magnetic field of 1 G. The typical response time (transit time) for such organic transistors is approximately $\tau_R \sim 4 \text{ ns}$.

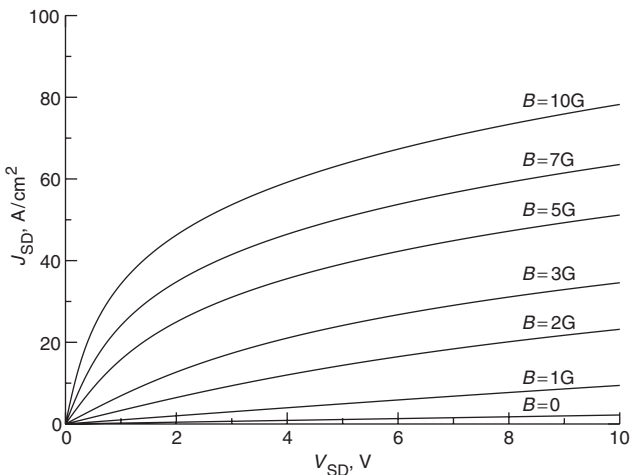


Fig. 5 Transistor current–voltage curves of antiparallel structure exposed to different magnetic fields
 $L = 5000 \text{ nm}$, $d = 200 \text{ nm}$ and $\nu = 1 \text{ cm}^2/\text{Vs}$

4 Conclusions

We have presented a theory to describe spin transport in magnet/polymer/magnet structures. This theory considers both the electric-field-induced spin drift and magnetic-field-induced spin precession and explains the observed magnetoresistance and I–V characteristics in LSMO/T₆/LSMO structures. We have also predicted that the interplay of spin drift and spin precession can give rise to damped oscillating

magnetoresistances with the transverse magnetic field in magnet/polymer/magnet structures. This theory provides a general framework to understand spin-dependent transport properties in polymer structures.

Based on this theory, we have proposed organic MFETs and ultrasensitive magnetometers that exploit spin transport in organics and its sensitive dependence on a transverse magnetic field due to spin precession. The organic MFETs can be operated under magnetic fields as weak as a few G with response times of a few ns. The organic ultrasensitive magnetometers can detect both a small magnetic field and a small magnetic-field change at sub-nT levels.

5 Acknowledgment

This work was partly supported by IRAD from SRI International.

6 References

- 1 Wolf, S.A., Awschalom, D.D., Buhrman, R.A., Daughton, J.M., von Molnar, S., Roukes, M.L., Chtchelkanova, A.Y., and Treger, D.M.: ‘Spintronics: A spin-based electronics vision for the future’, *Science*, 2001, **294**, pp. 1488–1495
- 2 Kikkawa, J.M., and Awschalom, D.D.: ‘Lateral drag of spin coherence in gallium arsenide’, *Nature*, 1999, **397**, pp. 139–141
- 3 Dediu, V., Murgia, M., Maticotta, F.C., Taliani, C., and Barbanera, S.: ‘Room temperature spin polarized injection in organic semiconductor’, *Solid State Commun.*, 2002, **122**, pp. 181–184
- 4 Xiong, Z.H., Wu, D., Vardeny, Z.V., and Shi, J.: ‘Giant magnetoresistance in organic spin-valves’, *Nature*, 2004, **427**, pp. 821–824
- 5 Campbell, I.H., and Smith, D.L.: ‘Physics of organic electronic devices’, *Solid State Phys.*, 2001, **55**, pp. 1–117
- 6 Yu, Z.G., Smith, D.L., Saxena, A., and Bishop, A.R.: ‘Green’s function approach for a dynamical study of transport in metal/organic/metal structures’, *Phys. Rev. B, Condens. Matter*, 1999, **59**, pp. 16001–16010
- 7 Lenz, J.E.: ‘A review of magnetic sensors’, *Proc. IEEE*, 1990, **78**, pp. 973–989
- 8 Qi, Y., and Zhang, S.: ‘Spin diffusion at finite electric and magnetic fields’, *Phys. Rev. B, Condens. Matter Mater. Phys.*, 2003, **67**, p. 052407
- 9 Aronov, A.G., and Pikus, G.E.: ‘Spin injection into semiconductors’, *Fiz. Tekh. Poluprovodn.*, 1976, **10**, pp. 1177–1179 (translated in *Sov. Phys. Semicond.*, 1976, **10**, pp. 698–700)
- 10 Yu, Z.G., and Flatte, M.E.: ‘Electric-field dependent spin diffusion and spin injection into semiconductors’, *Phys. Rev. B, Condens. Matter Mater. Phys.*, 2002, **66**, p. 201202
- 11 Yu, Z.G., and Flatte, M.E.: ‘Spin diffusion and injection in semiconductor structures: electric field effects’, *Phys. Rev. B, Condens. Matter Mater. Phys.*, 2002, **66**, p. 235302
- 12 Brataas, A., Nazarov, Y.V., and Bauer, G.E.W.: ‘Finite-element theory of transport in ferromagnetnormal metal systems’, *Phys. Rev. Lett.*, 2000, **84**, pp. 2481–2484
- 13 Hernando, D.H., Nazarov, Y.V., Brataas, A., and Bauer, G.E.W.: ‘Conductance modulation by spin precession in noncollinear ferromagnet normal-metal ferromagnet systems’, *Phys. Rev. B, Condens. Matter*, 2000, **62**, pp. 5700–5712
- 14 Yu, Z.G., Berding, M.A., and Krishnamurthy, S.: ‘Organic magnetic-field-effect transistors and ultrasensitive magnetometers’, *J. Appl. Phys.*, 2005, **97**, p. 024510
- 15 Yu, Z.G., Berding, M.A., and Krishnamurthy, S.: ‘Spin drift, spin precession, and magnetoresistance of noncollinear magnet-polymer-magnet structures’, *Phys. Rev. B, Condens. Matter Mater. Phys.*, 2005, **71**, p. 060408(R)
- 16 Bratkovsky, A.M., and Osipov, V.V.: ‘High-frequency spin-valve effect in a ferromagnet-semiconductor-ferromagnet structure based on precession of the injected spins’, *Phys. Rev. Lett.*, 2004, **92**, p. 098302
- 17 Bowen, M., Bibes, M., Barthelemy, A., Contour, J.P., Anane, A., Lemaitre, Y., and Fert, A.: ‘Nearly total spin polarization in La_{2/3}Sr_{1/3}MnO₃ from tunneling experiment’, *Appl. Phys. Lett.*, 2003, **82**, pp. 233–235
- 18 Cavallini, M., Biscarini, F., Dediu, V., Nozar, P., Taliani, C., Zamboni, R.: ‘Half metallic response of manganite films at room temperature from spin-polarized scanning tunneling microscopy’, *cond-mat/0301101*
- 19 Johnson, M., and Silsbee, R.H.: ‘Interfacial charge-spin coupling: injection and detection of spin magnetization in metals’, *Phys. Rev. Lett.*, 1985, **55**, pp. 1790–1793
- 20 Johnson, M., and Silsbee, R.H.: ‘Spin-injection experiment’, *Phys. Rev. B, Condens. Matter*, 1988, **37**, pp. 5326–5335
- 21 Jedema, F.J., Heersche, H.B., Filip, A.T., Baselmans, J.J.A., and van Wees, B.J.: ‘Electrical detection of spin precession in a metallic mesoscopic spin valve’, *Nature*, 2002, **416**, pp. 713–716

- 22 Strand, J., Schultz, B.D., Isakovic, A.F., Palmstrom, C.J., and Crowell, P.A.: 'Dynamic nuclear polarization by electrical spin injection in ferromagnet-semiconductor heterostructures', *Phys. Rev. Lett.*, 2003, **91**, p. 036602
- 23 Osipov, V.V., and Bratkovsky, A.M.: 'A class of spin injection-precession ultrafast nanodevices', *Appl. Phys. Lett.*, 2004, **84**, pp. 2118–2120
- 24 Tondra, M., Daughton, J.M., Wang, D., Beech, R.S., Fink, A., and Taylor, J.A.: 'Picotesla field sensor design using spin-dependent tunneling devices', *J. Appl. Phys.*, 1998, **83**, pp. 6688–6690
- 25 Pannetier, M., Fermon, C., Le Goff, G., Simola, J., and Kerr, E.: 'Femtotesla magnetic field measurement with magnetoresistive sensors', *Science*, 2004, **304**, pp. 1648–1650
- 26 Bandyopadhyay, S., and Cahay, M.: 'Proposal for a spintronic femto-tesla magnetic field sensor', *Physica E*, 2005, **27**, pp. 98–103